ASPECT RATIO- AND SIZE-CONTROLLED PATTERNED TRIANGULATIONS OF PARAMETRIC SURFACES

Oscar E. Ruiz
CAD CAM CAE Laboratory
EAFIT University
Cra. 49 No 7-sur-50
Medellin, Colombia
email: oruiz@eafit.edu.co

Sebastian Peña
Fraunhofer Inst. for Computer Graphics, Darmstadt, Germany
email: sebastian.pena.serna@igd.fraunhofer.de
Juan Duque
EAFIT University, Medellin, Colombia
email: jduquelo@eafit.edu.co

ABSTRACT
A method to produce patterned, controlled size triangulation of Boundary Representations is presented. Although the produced patterned triangulations are not immediately suited for fast visualization, they were used in Fixed Grid Finite Element Analysis, and do provide a control on the aspect ratio or shape factor of the triangles produced. The method presented first calculates a triangulation in the parameter space of the faces in which the B-Rep is partitioned and then maps it to 3D space. Special emphasis is set in ensuring that the triangulations of neighboring faces meet in a seamless manner, therefore ensuring that a borderless C^2 2-manifold would have as triangulation a C^0 borderless 2-manifold. The method works properly under the conditions (i) the parametric form of the face is a 1-1 function, (ii) the parametric pre-image of a parametric face is a connected region, and (iii) the user-requested sampling frequency (samples per length unit) is higher than twice the spatial frequency of the features in the B-Rep (thus respecting the Nyquist principle). As the conditions (i) and (ii) are possible under face reparameterization or sub-division and the condition (iii) is the minimum that a triangulation should comply with, the method is deemed as generally applicable.

KEY WORDS
2-Manifold Triangulation, Grid Triangulation, Constrained Delaunay, Parametric Space Triangulation

Glossary

$S(u,v)$	a parametric surface function. $S : R^2 \rightarrow R^3$. $S(u,v) = [x(u,v), y(u,v), z(u,v)]$
F	a FACE in a boundary representation.
F^{-1}	pre-image of F via $S(u,v)$: $S : F^{-1} \rightarrow F$.
L_F	set of loops of F. $L_F = \{L_0, L_1, ..., L_m\}$.
L_0	external loop of F.
L_i	internal loop of F ($i = 1, 2, ...$).
e	an edge of a loop of F.
p_i	point of e ($p_i \in F$).
(u,v)	parametric point in F^{-1}.
Γ_e	pre-image on F^{-1} of L_i.
Γ_L	pre-image on F^{-1} of L_F. $\Gamma_L = \{\Gamma_{e1}, \Gamma_{e2}..\}$
Δ_L	sampling distance measured on edges on F.
Δ_S	sampling distance measured on the interior of F.
T	Triangulation in 3D. Our final goal. Planar graph $T = (V, E)$ embedded in F.
T^{-1}	Triangulation in F^{-1}. Pre-image of T through S Planar graph $T^{-1} = (S^{-1}(V), E)$ in R^2.

1 Introduction

The issue of triangulating a Boundary Representation mounted on parametric surfaces and curves has been discussed in the literature. However, it is the aim of the present paper to present a simple, intuitive algorithm to triangulate such B-Reps. The algorithm discussed works correctly whenever the $S(u,v)$ and $C(u)$ mappings for the parametric surfaces and curves are 1-1 functions and the pre-image, in parametric space, of a trimmed surface is connected. These requirements are inherently present in the reviewed literature, although many authors fail to explicitly point it out. Our article also discusses the effects of violating such requirements. The present work reaches a valid, seamless, size controlled triangulation, which has been tested in the domain of Finite Element Analysis (Fixed Grid Methods), for which this type of triangulation is prepared. Once a valid triangulation is achieved, transformations on it can be produced, to satisfy other purposes (for example, fast rendering, level-of-detail, etc.). This article is divided into the following sections: a glossary section to identify the terms involved in the paper, a literature review, a methodology section which presents the strategy used, and a results and conclusions section, which discuses the limitations and strengths of the work and points out future work directions.

2 Literature Survey

Several classifications of the reviewed literature are possible: in the first place, [3], [7] and [8] treat the re-meshing of an already triangulated B-rep. Level of Detail is tangentially treated in [1], [8] and [10]. [4], [5] and [9] deal with the quasi-equilateral triangulation in F by iterative point search on $U \times V$ 2D parametric space. [2] and [6] pay special attention to the approximation of the face edges as

NURBS or Bezier curves in R^2.

In [1] an initial mesh is refined according to the disposition of the observer and the scene lights. An emphasis is set on multi-resolution only on the triangles that actually are seen by the observer. An directed acyclic graph (DAG) is formed, which tracks the modification operations performed on the vertices, edges or faces of a initial model. A Hausdorff distance between the reference and the current surfaces at the modified feature (edge, vertex, face) is evaluated, and the modifications are performed starting at sites with small value of such a measure (i.e. simplifications which only *slightly* modify the current surface when compared with the original one). The algorithms are designed to work in *image space* rather than in *object space*: subdivision is only performed if it does not surpass a threshold in the error introduced in the model, and it has an effect on the image. For example, if a triangle affects only one pixel there is no point in it being further subdivided.

In [2] an emphasis is set in producing watertight tessellations (borderless 2-manifolds in R^3) by using connectivity information. The face-face connectivity between the contiguous faces F_1 and F_2 is represented as a planar trimming curve $C_{1,2}(u)$ that is the common limit between the 2D regions (in parametric space $U-V$) that bound F_1 and F_2. A curvature-sensitive algorithm places vertices on the $C_{1,2}(u)$ curve. In the current article, the $C_{1,2}(u)$ curve is not required, as the implemented algorithm directly samples the edge curve in R^3 using the *curve* sampling interval specified by the user. In our algorithm, this sample on R^3 is tracked back to the $U-V$ plane by forming a piecewise linear approximation of the trimming curve $C_{1,2}(u)$.

In [3], the authors start with a watertight 2-manifold M with C^0-continuity (a triangulated tessellation), and build a set of parameterizations for M. Each parameterization covers what is called an *internal node* (representing an M_i 2-manifold with border) in the Reeb Graph describing the topological chances in M along the range of a Morse function $f : M \longrightarrow R$. As per the Morse theory, M_i represents a portion of the M manifold, for which f has no singular points (topological changes of M) and therefore represents the complete log of the topological evolution of M. Four types of M_i are possible: cylinders, cups, caps, and branchings, according to the borders of M_i. For each type, a pre-defined routine is used, which parameterizes M_i. The step of making compatible the parameterizations for $M_i, i = 0, 1, 2, ...$ is avoided by remeshing the parameterizations with higher density at the borders of M_i. In this form, still a series of parameterizations is possible, while guaranteeing a watertight remeshed M_r version of M.

In [4] and [5] a parameterization-independent algorithm is proposed to triangulate a surface. The aim of the authors is to produce a nearly uniform triangulation. That is, a triangulation in which the triangles be quasi-equilateral. A vertex $p = S(u_0, v_0)$ is chosen on $S(u, v)$ and the plane tangent to S at p, $T_p(p)$, is calculated. On $T_P(p)$, a circle with radius R and its regular inscribed polygon with n sides (called Normal Umbrella - NU) are constructed along with the n incident triangles covering the 2Π angle around p. Each angle that contributes to 2Π is projected onto S, with vertex $p = S(u_0, v_0)$ and projection rays perpendicular to $T_p(p)$. The radius R is inversely proportional to the local curvature.

In [6] the display of a trimmed NURBS face is discussed, in which a *compilation* stage is performed. The compilation stage is equivalent to what other authors call *the triangulation*. The face in parametric UV space corresponds to a 2D connected region with holes, bounded by curved Bezier approximations of the NURBS trimming curves. Bezier approximations are used because there exist reasonable algorithms for the finding of a root of a Bezier curve. The region in UV space is cut into sub-regions which have monotonically increasing or decreasing values of the U and V parameters. These subregions are triangulated separately. As an improvement, the algorithm implemented in this paper avoids the splitting of the UV region into subregions. It also requires only linear intersections (not Bezier ones), leading to a very simple implementation.

[7] presents a mesh-improving method that starts with a topologically valid although geometrically poor triangular mesh. The geometric degeneracies are classified as *needles* (quasi isosceles triangles that have two vertices very close to each other) and *caps* (triangles with one angle very close to $180°$). The elimination of needles is relatively simple. Elimination of each cap requires the slicing of the *whole* mesh along a particular plane, producing an overpopulation of triangles. The distance between the final and initial triangulations is used to accept or reject the cap and needle elimination. [8] starts from reverse engineering or tessellation triangular meshes to execute quality improvement and property control on them. The article applies the subdivision and simplification functions to augment and diminish the degree of freedom of the mesh, respectively. Several heuristics are applied to refine the mesh: geometric error, face size, faces shape quality, edge size and vertex valence. In neither [7] nor [8] the mesh modifications are evaluated against the original solid, but against an existing triangulation of it. A comparison with our article is not possible, since our work seeks an initial triangulation for a given solid.

[9] propose a quasi - isometric local mapping from a parametric surface $S(u, v) : U \times V \rightarrow R^3$ by using the control polyhedron (called there the *surface net*) of the parametric surface. The reasoning is that the surface net closely follows the warping of the parametric surface, while at the same time is very similar to a *locally* developable surface (in turn a planar surface). If we assume that a 1-1 function $f : U \times V \rightarrow S_D \subset R^2$ is known (S_D is the developed surface net), then a quasi equilateral triangulation could be calculated on S_D, and taken to the $U \times V$ domain by using f^{-1}. From $U \times V$ the triangulation is taken to R^3 by using the parametric equations $S(u, v)$. The image in $U \times V$ of the quasi equilateral triangles in S_D is not quasi-equilateral, but their image in R^3 would be. The paper presents no examples in which S_D does not exist for

the original surface, and a subdivision must be done, but mentions this possibility.

[10] discusses the issue of triangulation a trimmed surface F by sub-dividing a rectangular domain in the $U \times V$ space using Quadtrees. Each quadtree is recursively subdivided if its corner points in R^3 deviate from a plane beyond a prescribed limit. The trimming NURBS curves, which limit the face F to triangulate are represented as piecewise linear in R^3 and in the parametric $U \times V$ space also. The quadtrees which are completely inside the piecewise linear boundary are trivially triangulated. The ones cut by a loop segment are triangulated only in its internal extent. The quadtree portions in $U \times V$ external to the boundary loops are not triangulated. The paper mentions but does not discuss a process of conciliation between the triangulations of adjacent faces in order to have a seamless triangulation at the faces boundaries.

[11] and [12] are quite important references, used in this paper, regarding the triangulation of 2D regions. In the present work, a Constrained Delaunay Triangulation was used, which respects prescribed edges defined on a set of planar points.

3 Methodology

A triangulation is a connected, non directed, planar graph $G = (V, E)$ of vertices V and edges E whose cycles of length 3 exhaust all edges. There are no cycles with length smaller than 3. Every vertex has degree greater than 1. The planarity of the graph is independent on the dimension of the space in which it is embedded. In particular, a graph embedded in R^2 may be planar or non-planar.

The following steps produce the required triangulation: Since the triangulation is a planar graph, the solution method is (a) to find a 1-1 function g which maps F onto a region $F^{-1} \subset R^2$, (b) to calculate the triangulation T^{-1} on F^{-1} with well known triangulation algorithms (in this case one uses *Triangle* [11]), and (c) to map T^{-1} back onto $F \subset R^3$, by using g^{-1}.

3.1 Inverse Map

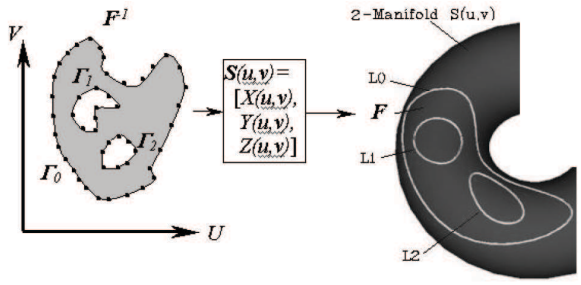

Figure 1. Forward Map $S(u, v)$ from $F^{-1} \subset R^2$ onto F

Several functions g were tested. Among them, parallel projections of F onto a plane. However, these functions were discarded since in cases of highly curved Fs it is impossible to find a suitable projection plane which leads to a 1-1 function. Instead (see Figure 1) the function g was chosen to be $g = S^{-1} : R^3 \rightarrow U \times V$, or equivalently, $g^{-1} = S : U \times V \rightarrow R^3$. Notice that it is still required that S be a 1-1 function. Therefore this solution method does not apply for carrier surfaces $S(u, v)$ for which $S(u_1, v_1) = S(u_2, v_2)$ with $(u_1, v_1) \neq (u_2, v_2)$ The steps of the solution are discussed next.

3.2 Calculation of F^{-1}

The first step is to calculate the region $F^{-1} \in R^2$, that is, the pre-image of F under the parametric surface $S(u, v)$. F^{-1} is the connected region (possibly with holes) in R^2 bounded by an external curve Γ_0 and internal ones $\Gamma_i, i = 1, ...$ The following algorithm approaches the Γ_i as Piecewise Linear curves. They constitute the *constrained triangle edges* for triangulation T^{-1}.

function Calculation of F^{-1}(Δ_L, L_F, S)
Δ_L : Sampling Distance, L_F : Loops of Face F,
S: Carrier surface for F

{
make $F^{-1} = []$
for loop $L \in L_F = \{L_0, L_1, ..., L_m\}$
  Make $\Gamma_L = []$
  for edge $e \in EDGES(L)$
    Find $P = \{p_1, p_2, .., p_{n_e}\}$ a sample of e
    with intervals of size Δ_L
    Make $\Gamma_e = \{(u_1, v_1), (u_2, v_2), ..., (u_{n_e}, v_{n_e})\}$
    such that $(u_i, v_i) = S^{-1}(p_i), i = 1...n_e$
    Make $\Gamma_L = [\Gamma_L, \Gamma_e]$
  end
  Make $F^{-1} = [F^{-1}, \Gamma_L]$
end
Orient L_0 in CCW sense with respect to $(0, 0, 1)$
Orient $L_1, L2, ..., L_m$ in CW sense with respect to $(0, 0, 1)$
}

3.3 Calculation of Triangulation T^{-1} on F^{-1} (space $U \times V$)

As F^{-1} is a planar region in space $U \times V$, a triangulation of it may be easily generated with a 2D-triangulation Algorithm. The algorithm chosen is the one by Jonathan Shewchuk ([11]), and implemented in the *Triangle* package. This algorithm allows to set up priorities in the triangles built to cover F^{-1}: to generate (a) *quality* triangles (i.e. with restriction on their acuteness), or (b) triangles having prescribed edges (in our case, the ones generated in the step before), called *constrained triangle edges*. The present case is of the type (b), in which the triangulation vertices are the ones described in the last section.

3.3.1 Generation of Internal Vertices for T^{-1}

A uniform grid of vertices are generated in the interior of the region F^{-1} (Figure 2). The interval for this resample of a 2-manifold is Δ_S (independent of Δ_L, the interval for 1-manifold sampling). Δ_S must also be compliant with the Nyquist criterion for digital sampling of an analogue phenomenon. An effect of the compliance with the Nyquist criterion is that as the edges so formed are *forced* to become nodes of the triangulation graph (this is exactly the function of a constrained triangle edge), the connectivity and quality of the triangulation are controlled. Loose sampling intervals Δ_S and Δ_L in generating the T^{-1} triangulation produce topologically illegal, possibly non planar, triangulations.

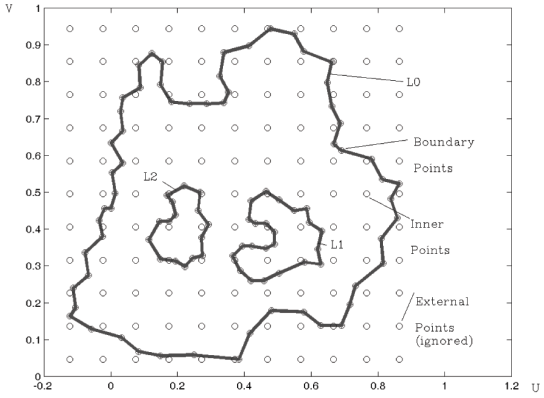

Figure 2. F^{-1} and Boundary Vertices in $U \times V(R^2)$ Space

Figure 2 shows the (in this example) three loops L_0, L_1 and L_2 bounding the F^{-1} region. Also, a patterned grid of vertices is easily generated by using the bounding box of L_0 in $U \times V$. This grid includes *inner*, *border* and *external* points, from which the later ones are not considered in generating the triangulation for the region.

Figure 3 shows the triangulation achieved in $U \times V$ space for the level of resolution of this example (Δ_L). As evident from the figure, the patterned grid of internal points must be fine enough to force the triangulation to form triangles reaching the boundary of $F^{-1]}$.

3.4 Map of 2D (T^{-1}) Triangulation into 3D (T)

The mapping of the triangulation $T^{-1} = (V^{-1}, E^{-1})$ lying on the $U \times V$ plane into 3D space (the parametric surface $S(u, v)$) is easily done by evaluating each point of the triangulation (u_i, v_i) in the function $S(u_i, v_i) = [X(u_i, v_i), Y(u_i, v_i), Z(u_i, v_i)]$. Therefore, the $T = (V, E)$ triangulation in R^3 is defined as: (i) the set of nodes on F are calculated as $V = S(V^{-1})$, (b) an edge $e = (S(v_i), S(v_j)) \in E$ iff the edge $e^{-1} = [v_i, v_j] \in E^{-1}$

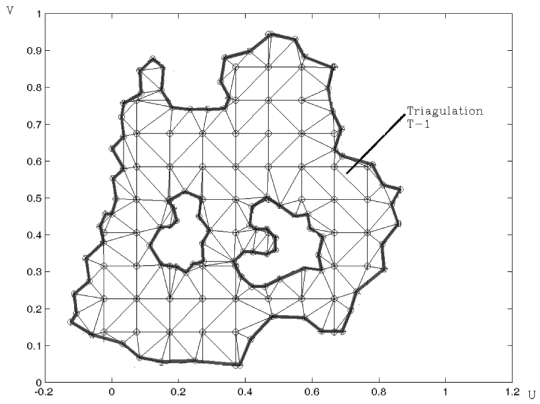

Figure 3. Triangulation T^{-1} in $U \times V(R^2)$ Space

; that is, if the pre-images of nodes $S(v_i)$ and $S(v_j)$ are joined by an edge in E^{-1}.

4 Results and Conclusions

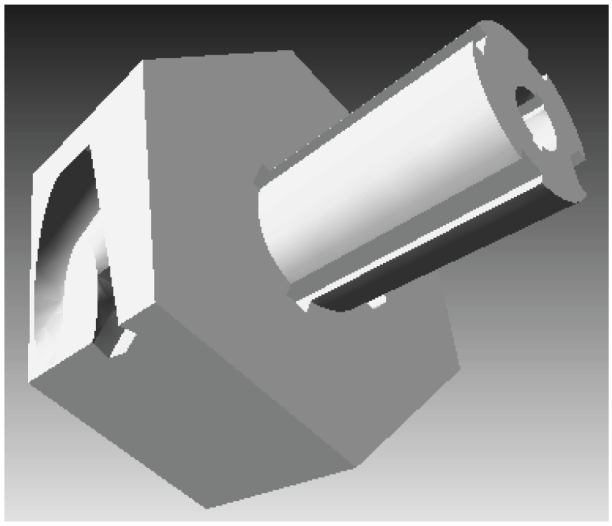

Figure 4. Tester 4. Render

Figures 4 to 7 show the back mapping from the triangulation T^{-1} in $U \times V$ in 2-dimensional space onto T on F (3D) by using the parametric function $S(u, v)$. Several comments are relevant at this point:

1. The resulting triangulation $T = (V, E)$ is a correct C^0 *watertight* (that is, *borderless*) 2-manifold, if constrained triangle edges are specified, as done in our work. When the triangulation is a *quality* one, no constrained triangle edges are allowed, and the triangles are defined based on aspect ratio criteria alone. In

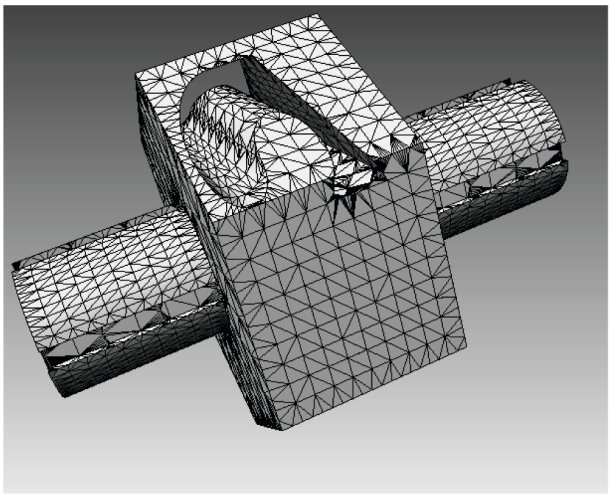

Figure 5. Tester 4. Triangulation

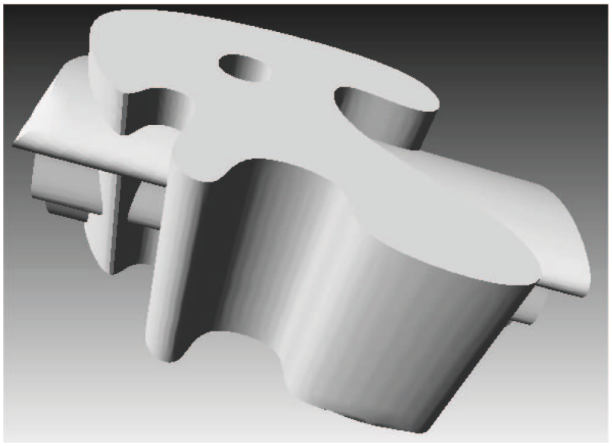

Figure 6. Tester Spline. Render

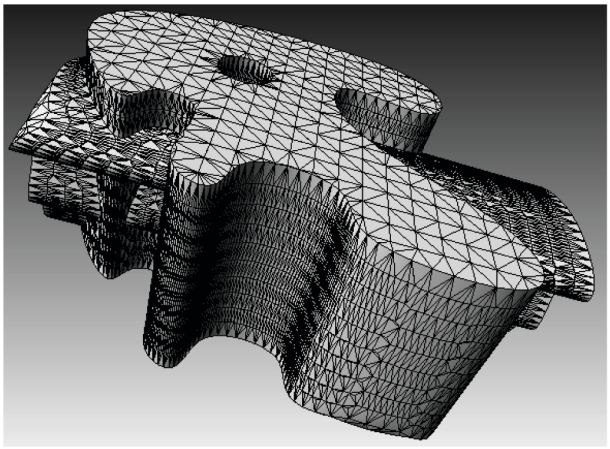

Figure 7. Tester Spline. Triangulation

this case there is obviously no guarantee of a seamless union between face F and its neighbours $F_i, i = 1, ...$

2. The sampling intervals Δ_L and Δ_S are defined, as expected, by the Nyquist criterion: they must be smaller than half of the minimal characteristic distance of the feature D_F to appear in the triangulation. It must be kept in mind that a triangulation $T = (V, E)$ is nothing different from the 1-order hold digital sample of the original B-Rep. As such, Δ_L and Δ_S must be sufficiently fine to preserve the desired detail. From Figures 4 to 7 is also visible that Δ_L and Δ_S are independent from each other.

3. Because of the insertion of constrained triangle edges, the triangulation $T^{-1} = (V^{-1}, E^{-1})$ *cannot* be a Delaunay one, but a *Constrained Delaunay Triangulation - CDT*. This is required to guarantee a seamless or watertight triangulation at the faces borders.

4. Figure 8 shows how the fact of $S(u, v)$ not being a 1-1 function leads to wrong results in calculating the pre-image of the F cylindrical surface. The interrogation of the $S(u, v)$ surface gives $(0, \pi) = S^{-1}(J)$ **and** $(0, \pi) = S^{-1}(B)$ ([13]). The correct result, namely $(0, -\pi) = S^{-1}(B)$ is not calculated because $S(0, \pi) = S(0, -\pi) = B = J$ (not a 1-1 function) and therefore S^{-1} does not exist. As a result, Γ_0 happens to be a degenerated polygon, producing the F^{-1} area to vanish.

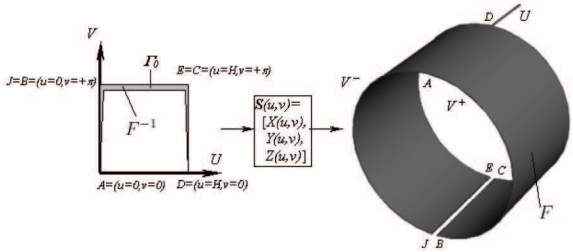

Figure 8. Wrong calculation of F^{-1} in $U \times V(R^2)$ caused by $S(u, v)$ not being 1-1.

5. Figure 9 shows another aberration produced by F^{-1} being unconnected (made possible by $S(u, v)$ not being 1-1). The half cylinder F is **one** connected face in the Boundary Representation. The v parameter in the underlying surface $S(u, v)$ ranges in $[-\pi, \pi]$. Therefore, $S(u, \pi) = S(u, -\pi), \forall u \in [0, H]$ (not a 1-1 function). Mapping back F via S^{-1} renders an unconnected F^{-1}, if S^{-1} could be correctly calculated. If that is not the case (see previous item), the Γ_0 polygon is self-intersecting.

   It should be pointed out that $S(u, v)$ being 1-1 and F^{-1} being connected are conditions that are underlying in all the reviewed literature, although many au-

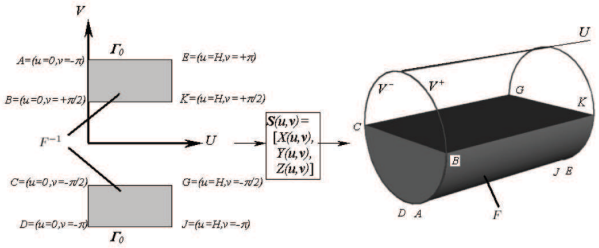

Figure 9. Disconnection of F^{-1} in $U \times V(R^2)$ space.

thors fail to point them out. In our case, it is clear that those are necessary conditions for our method to work properly.

6. An application of triangulations in Fixed Grid Methods (an alternative to traditional Finite Element Analysis) is shown in Figure 10. In such a method the produced triangulation is immersed into a fixed grid. More information on such immersion process and the Fixed Grid methods may be found in [14] and [15].

Figure 10. Piston Triangulation and FEA Simulation

7. Future Work includes two main aspects:

   (a) The triangulation $T = (V, E)$ obtained is overly detailed in the borders and on flat faces. Hence, starting from the 2-manifold without border $T = (V, E)$, a relaxation is required to minimize the size of T for a given permissible deviation between T and F.

   (b) The procedure implemented is a correct one as long as $S(u, v) : R^2 \rightarrow R^3$ is a 1-1 function. The reason for such a request is obviously the intensive use made of the $S^{-1}(p)$ function ($p \in F$), specifically in the calculation of the F^{-1} region connected region in the $U \times V$ space. If $S(u, v)$ is not a bijection the F^{-1} region may have self-intersecting boundary, zero area (8) or may be disconnected (9). Future work on these cases is required.

Acknowledgement

The present work was founded by the Colombian Council for Science and Technology (Colciencias) under project CAD-FixGrid 572-2003.

References

[1] R. Klein, A. Schilling and W. Strasser, Illumination Dependent Refinement of Multiresolution Meshes, *Proc. Computer Graphics International CGI'98*, Los Alamitos, CA, USA, 1998, 680-687.

[2] W. A. G. Stöger and G. Kurka, Watertight Tessellation of B-rep NURBS CAD-Models using connectivity information, *Intl. Conf. on Imaging Science, Systems and Technology, CISST '03*, Las Vegas, USA, 2003, 602-606.

[3] G. Patanè, M. Spagnuolo and B. Falcidieno, Para-Graph: Graph-Based Parameterization of Triangle Meshes with Arbitrary Genus, *Computer Graphics Forum*, 23(4), 2004, 783-797.

[4] M. Attene, B. Falcidieno, M. Spagnuolo and G. Wyvill, Mapping Independent Triangulation of Parametric Surfaces, *Intl. Conf. on Shape Modeling and Applications 2002 (SMI'02)*, Banff, Canada, 2002, 67-74.

[5] M. Attene, B. Falcidieno,M. Spagnuolo and G. Wyvill, A mapping-independent primitive for the triangulation of parametric surfaces, *Graphical Models*, 65(5), 2003, 260-273.

[6] S. Abi-Ezzi and S. Subramaniam, Fast Dynamic Tessellation of Trimmed NURBS Surfaced, *Computer Graphics Forum*, 13(3), 1994, 107-126.

[7] M. Botsch and L. Kobbelt, Robust Procedure to Eliminate Degenerate Faces from Triangle Meshes, *Proc. Vision, Modelling and Visualization (VMV01)*, Stuttgart, Germany, 2001, 283-289.

[8] H. Date, S. Kanai, T. Kishinami, I. Nishigaki and T. Dohi, High Quality and Property Controlled Finite Element Mesh Generation from Triangular Meshes using Multiresolution Technique, *ASME Journal of Computing and Information Science in Engineering*, 5(4), 2005, 266-276.

[9] W. Cho, N. M. Patrikalakis and J. Peraire, Approximate Development of Trimmed Patches for Surface Tessellation, *Computer Aided Design*, 30(14), 1998, 1077-1087.

[10] C. Shu and P. Boulanger, Triangulating Trimmed NURBS Surfaces, *International Conference on Curves and Surfaces*, Saint-Malo, France, 2000, 381 - 388.

[11] J. Shewchuk, Delaunay Refinement Algorithms for Triangular Mesh Generation, *Computational Geometry: Theory and Applications*, 22(1), 2002, 86-95.

[12] J. Shewchuk, *General-Dimensional Constrained Delaunay and Constrained Regular Triangulations I: Combinatorial Properties* (Tech. Report, U. California Berkeley, 2005).

[13] Spatial Techn. Inc., *ACIS 3D Toolkit. Technical Overview*, (Boulder, USA, Spatial Technology Inc. 3D/Eye Inc., 1995).

[14] O. Ruiz, M. Granados and C. Cadavid, FEA-driven Geometric Modelling for Meshless Methods, *Proc. Virtual Concept*, Biarritz, France, 2005, 1-8.

[15] M. Garcia, M. Henao and O. Ruiz, Fixed Grid Finite Element Analysis for 3D Structural Problems, *Intl. J. of Computational Methods* , 2(4), 2005, 569-585.